



**CHALMERS**  
UNIVERSITY OF TECHNOLOGY

## **Kinetics of Reaction on a Single Catalytic Particle in a Fluidic Nanochannel**

Downloaded from: <https://research.chalmers.se>, 2026-04-06 16:05 UTC

Citation for the original published paper (version of record):

Zhdanov, V. (2020). Kinetics of Reaction on a Single Catalytic Particle in a Fluidic Nanochannel. *Catalysis Letters*, 150(6): 1749-1756. <http://dx.doi.org/10.1007/s10562-019-03082-1>

N.B. When citing this work, cite the original published paper.



# Kinetics of Reaction on a Single Catalytic Particle in a Fluidic Nanochannel

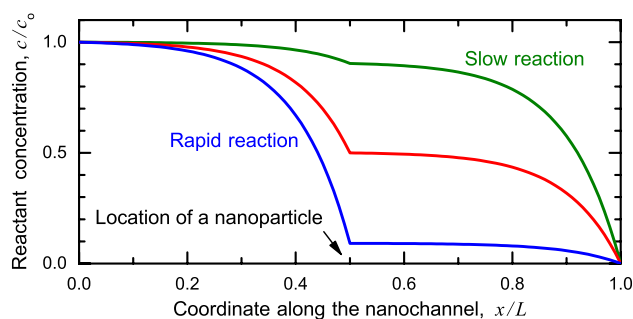
Vladimir P. Zhdanov<sup>1,2</sup>

Received: 22 October 2019 / Accepted: 13 December 2019 / Published online: 27 December 2019  
© The Author(s) 2019

## Abstract

One of the frontiers in heterogeneous catalysis is focused on reactions occurring on single catalytic nanoparticles. In this context, a reaction taking place on a single nanoparticle in a fluidic nanochannel is herein described by using the equation similar to that employed for a plug-flow reactor with dispersion. In the literature, one can find various boundary conditions for this equation. In the practically interesting case of a relatively long channel, the Dirichlet boundary conditions are shown to be valid. The corresponding analytical and numerical results illustrate the specifics of the profiles of the reactant concentration along the channel and the dependence of the reaction rate on the parameters. For comparison, the Danckwerts boundary conditions were used as well.

## Graphic Abstract



**Keywords** Reaction kinetics · Single catalytic nanoparticle · Fluidic nanochannel · Dirichlet and Danckwerts boundary conditions

## 1 Introduction

In chemical engineering, there are a few basic types of chemical reactors including an ideal batch reactor, continuous stirred-tank reactor (CSTR), plug-flow reactor (PFR; or, in other words, cross-flow or fixed-bed reactor), and more specific reactors such e.g. as semibatch reactor, distillation

reactor, PFR with distributed feed, and recirculation reactor [1]. In all these reactors, chemical conversion occurs in every part of a reactor. Reactors with locally occurring reaction are also possible. In the temporal analysis of products reactor (TAPR), for example, reaction takes place locally and conversion is proportional to the difference between inlet and outlet diffusional fluxes [2]. The generic kinetic models describing such reactors are usually simple and often focused on a first-order reaction. Despite this simplicity, such models were and are widely used in various contexts.

The reactors mentioned above are employed in chemistry in general and heterogeneous catalysis in particular. In the latter area, chemical reactions are well known to

✉ Vladimir P. Zhdanov  
zhdanov@chalmers.se

<sup>1</sup> Section of Chemical Physics, Department of Physics, Chalmers University of Technology, Göteborg, Sweden

<sup>2</sup> Boreskov Institute of Catalysis, Russian Academy of Sciences, Novosibirsk, Russia

occur usually on nanoparticles (NPs) located on the walls of pores inside a support [3]. For advances in modelling of reactors for such reactions, one can read recent review [4]. The related academic kinetic studies have long been focused on reactions running on single-crystal surfaces [5, 6] and supported 2D arrays of NPs [7]. One of the new directions in this area is aimed at reactions occurring on single NPs (see, e.g., Refs. [8–12]). For reactions in the liquid phase, one of the related generic schemes (Fig. 1) includes a nanofluidic channel with reactant diffusion occurring in liquid flow and with a catalytic NP located inside [12]. In this Letter, I present and analyze the simplest generic analytical one-dimensional (1D) kinetic model allowing one to clarify what may happen in such situations under steady-state conditions. The model proposed takes flow and diffusion of reactant into account, and these ingredients are similar to those used to describe PFR with dispersion (see, e.g., Ref. [13]). The difference is that in the case under consideration the reaction is considered to occur locally whereas in the PFR case it takes place along the whole reactor. There are also similarities with the 1D model describing TAPR [14] where reaction occurs locally. The TAPR model does not, however, take reactant flow into account.

Basically, the system shown schematically in Fig. 1 represents a new type of catalytic reactors or an extended version of the TAPR reactor. By analogy with the CSTR, PFR, and TAPR cases, the generic analytical 1D model of the reactor under consideration is expected to be useful for clear understanding of the principles of its function and the profiles of reactant concentrations inside. One can of course use more complex 2D or 3D models of this reactor and analyze them numerically (see, e.g., Refs. [15–17] for various related aspects). All these (1D, 2D, and 3D) models are complementary and their applications depend on circumstances.

## 2 Analysis

### 2.1 General Kinetic Equations

In the model I use (Fig. 1), the nanofluidic channel is considered to be relatively long so that its length,  $L$ , is much larger than the size (effective radius),  $a \equiv (s/\pi)^{1/2}$ , characterizing its cross section perpendicular to its axis ( $s$  is the cross-section area). The concentration of reactant is assumed to be low so that its diffusion is ideal and conversion does not change the flow rate of solution. In addition, the size of a catalytic NP is considered to be small compared to  $a$ , and accordingly its presence does not change the solution flow either. In this case, the solution flow in and the reactant distribution along the channel can be described by employing the 1D approximation. In particular, the reactant concentration,  $c$ , can be defined as the number of molecules per unit length. According to this definition, one has  $c = sC$ , where  $C$  is the conventional concentration calculated per unit volume. The suitable 1D equation for the reactant concentration takes diffusion and flow into account,

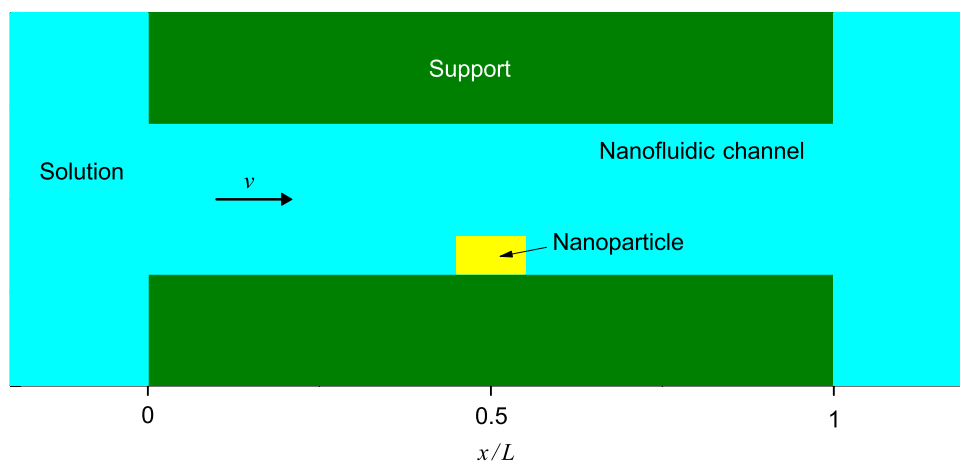
$$\frac{\partial c}{\partial t} = D \frac{\partial^2 c}{\partial x^2} - v \frac{\partial c}{\partial x} - w(c), \quad (1)$$

where  $D$  is the reactant diffusion coefficient,  $v$  is the flow velocity related to the pressure drop (in reality, this is the flow velocity averaged over the channel cross section),  $w(c)$  is the reaction rate, and  $0 \leq x \leq L$  is the coordinate along the channel. Under steady-state conditions, this equation is reduced to

$$D \frac{\partial^2 c}{\partial x^2} - v \frac{\partial c}{\partial x} = w(c). \quad (2)$$

In chemical engineering, Eq. (1) [or (2)] is usually used to describe PFR (with dispersion) where a reaction occurs along the whole reactor. In the situation under consideration,

**Fig. 1** Scheme of a fluidic nano-channel with a single catalytic nanoparticle



in contrast, the reaction is considered to take place on a single catalyst NP located inside the reactor (Fig. 1). Mathematically, the reaction rate can in this case be represented as the delta function,

$$w(c) = w_p(c(x_p))\delta(x - x_p), \quad (3)$$

where  $w_p(c(x_p))$  is the total reaction rate at the NP, and  $c(x_p)$  is the reactant concentration at the NP location. With this specification, Eq. (2) reads as

$$D \frac{\partial^2 c}{\partial x^2} - v \frac{\partial c}{\partial x} = w_p(c(x_p))\delta(x - x_p). \quad (4)$$

At  $0 \leq x < x_p$  and  $x_p < x \leq L$ , Eq. (4) is reduced to

$$D \frac{\partial^2 c}{\partial x^2} - v \frac{\partial c}{\partial x} = 0. \quad (5)$$

The suitable general solution of the latter equation is

$$c(x) = [A - B \exp(vx/D)]c_0 \quad \text{at } 0 \leq x < x_p, \quad \text{and} \quad (6)$$

$$c(x) = [F - E \exp(vx/D)]c_0 \quad \text{at } x_p < x \leq L, \quad (7)$$

where  $c_0$  is the inlet reactant concentration (i.e., the concentration in the solution supplied into the channel), and  $A$ ,  $B$ ,  $E$ , and  $F$  are positive dimensionless constants determined by the reaction conditions at  $x = x_p$  and the boundary conditions at  $x = 0$  and  $x = L$ .

To validate the use of the 1D approximation in the model introduced above, I can add to remarks. The first one concerns the regions which are not just near a NP. In these regions, the time scale of reactant diffusion in the direction perpendicular to the channel axis is much shorter than that for diffusion along the channel because the channel is long. Under such circumstances, the reactant-concentration gradients in the direction perpendicular to the channel axis are negligible. This argument is the same as in the case of conventional PFRs.

Concerning the regions just near a NP, one can distinguish two apparently different situations. (i) If the reaction is there kinetically controlled, the reactant-concentration gradients are negligible. (ii) If the reaction is there controlled by diffusion, the local gradients of concentration can be appreciable, but only at the length scale comparable with the NP size, and the reaction rate will be proportional to the local concentration in the area slightly outside the region just near the NP, i.e., the reaction will be of first order. Practically, this means that the reaction rate will anyway be determined by local reactant concentration in both cases [(i) and (ii)]. The difference may be only in the reaction order and the value of the corresponding reaction rate constant. In other words, this means that the model is applicable in both cases, especially for first-order reactions.

## 2.2 Reaction Conditions

With the reaction taking place at  $x = x_p$ , there are two conditions. First, the concentration should be continuous, i.e., one should have

$$A - B \exp(vx_p/D) = F - E \exp(vx_p/D). \quad (8)$$

The second condition can be obtained by integrating Eq. (4) from  $x = x_p^-$  to  $x = x_p^+$ ,

$$D \frac{\partial c}{\partial x} \Big|_{x_p^+} - D \frac{\partial c}{\partial x} \Big|_{x_p^-} = w_p(c(x_p)). \quad (9)$$

Using (6) and (7), the latter condition can be rewritten as

$$vc_0(B - E) \exp(vx_p/D) = w_p([F - E \exp(vx_p/D)]c_0). \quad (10)$$

This equation can be employed in order to relate  $B$ ,  $E$ , and  $F$  provided the dependence of the reaction rate,  $w_p(c)$ , on  $c$  is explicitly defined.

To illustrate typical profiles of the reactant concentration, I will use below the first-order reaction with

$$w_p(c) = w_0 c, \quad (11)$$

where  $w_0$  is the reaction rate constant.

## 2.3 Boundary Conditions

In general, the boundary conditions at the inlet ( $x = 0$ ) and outlet ( $x = L$ ) are not unique and should be formulated by scrutinizing the details of the reactant flow on both sides of each boundary. Axiomatically, one can introduce at least two types of boundary conditions.

In particular, the Dirichlet boundary conditions (see, e.g., Ref. [14]) are given by

$$c(0) = c_0, \quad (12)$$

$$c(L) = 0. \quad (13)$$

Physically, these conditions imply that the reactant concentration at the boundaries is continuous. Specifically, the former condition means that the concentration at  $x = 0^+$  is equal to the inlet concentration at  $x = 0^-$ . The latter condition is based on the assumption that the reactant is fully absorbed at  $x = L^+$ , and accordingly its concentration can be set to zero at  $x = L^-$ .

The Danckwerts boundary conditions are formulated as [18]

$$vc(0) - D \frac{\partial c}{\partial x} \Big|_{x=0^+} = vc_0, \quad (14)$$

$$\left. \frac{\partial c}{\partial x} \right|_{x=L^-} = 0. \quad (15)$$

The first condition implies that the total reactant flux at  $x = 0^+$  is equal to the input flux determined by the solution velocity. The second condition means that the diffusion flux at  $x = L^-$  is negligible. For a few examples of the application of these boundary conditions, I may mention Refs. [13, 19, 20].

In the chemical engineering literature, one can find a few discussions on the pros and cons of the use of various boundary conditions in the context of modelling a plug-flow reactor with dispersion. In particular, Mott and Green [21] note with suitable references that there was/is criticisms concerning the concentration jump at the inlet boundary according to Danckwerts' condition (14) and that no authors of contemporary chemical reaction engineering texts are willing to employ Danckwerts' boundary conditions. With this reservation, they themselves are in favour of these conditions.

For reaction in a fluidic nanochannel, the Dirichlet boundary conditions appear to be preferable. To validate the use of these conditions, let us consider and compare various fluxes e.g. near the left-hand-side channel boundary (Fig. 1). In particular, let us choose two surfaces. One, with area  $s$ , is that corresponding to the channel boundary at  $x = 0$ . The second one is a hemisphere (with radius  $\rho = 1.5a$  [ $a \equiv (s/\pi)^{1/2}$ ]) located outside the channel boundary and with the basis contacting this boundary so that the boundary is located in the center of the basis. The important point here is that the space filled by solution at  $x < 0$  (to the left from the nanochannel) is much larger than the nanochannel. In this case, the diffusion-related gradients of the reactant concentration near the channel at  $x < 0$  takes place on the length scale of  $\rho$ . This means that the reactant concentration at the hemisphere is close to that,  $C_0$ , in the solution far from the channel [this concentration and the concentration  $C(0)$  below are conventional and defined as the number of molecules per unit volume]. (i) The scale of the hydrodynamic reactant flux crossing the hemisphere is accordingly  $2\pi\rho^2v_{\text{hs}}C_0$ , where  $v_{\text{hs}}$  is the average solution velocity there. In reality, the solution is nearly non-compressible, and accordingly  $2\pi\rho^2v_{\text{hs}} = \pi a^2v$ , where  $v$  is the solution velocity at the channel boundary, which is the same as that in the channel (the latter velocity is used in the bulk of the equations above and below). Thus, this flux is equal to  $\pi a^2vC_0$ . (ii) The scale of the reactant diffusion flux across the hemisphere is  $2\pi\rho^2D[C_0 - C(0)]/\rho$ , or  $2\pi\rho D[C_0 - C(0)]$ , or  $3\pi aD[C_0 - C(0)]$ , where  $C(0)$  is the reactant concentration at the channel boundary, i.e., at  $x = 0$ . (iii) The hydrodynamic reactant flux crossing the channel boundary is  $\pi a^2vC(0)$ . (iv) The scale of the reactant diffusion flux across the channel boundary is  $\pi a^2DC(0)/\lambda$ , where  $\lambda$  is the length scale

characterizing the drop of the concentration in the channel near the boundary. These four fluxes should be balanced,

$$\pi a^2vC_0 + 3\pi aD[C_0 - C(0)] \simeq \pi a^2vC(0) + \pi a^2C(0)/\lambda, \quad \text{or} \\ v[C_0 - C(0)] + 3\pi D[C_0 - C(0)]/a \simeq DC(0)/\lambda. \quad (16)$$

The length  $\lambda$  is comparable with or larger than the channel length,  $L$ , which in turn is considered in our analysis to be much larger than  $a$ . Under such circumstances, condition (16) can be satisfied only provided  $C(0)$  is very close to  $C_0$ , i.e., one can use  $C(0) = C_0$ . Multiplying the left and right parts of the latter condition by  $s$  ( $s \equiv \pi a^2$ ) yields (12). Condition (13) can be validated in a similar way.

Concerning boundary conditions (13) and (15), I can add that their applicability depends on the details of the fluid removal at the outlet. Condition (13) is applicable provided the removal is rapid and irreversible so that there is no reactant diffusion from the region outside the channel ( $x > L$ ) back to the region inside the channel ( $x < L$ ). If the region outside the channel ( $x > L$ ) represents another channel so that reactant diffusion back to the main channel is possible, condition (15) may be preferable.

The analytical and numerical results obtained with the Dirichlet boundary conditions (12) and (13) are presented just below (Sect. 2.4). For comparison, the results obtained with the Danckwerts boundary conditions (14) and (15) are presented as well (Sect. 2.5).

## 2.4 With the Dirichlet Boundary Conditions

In this subsection, the reaction kinetics is described by using expressions (6) and (7) for the reactant concentration, boundary conditions (12) and (13) at  $x = 0$  and  $x = L$ , and reaction conditions (8) and (10) at  $x = x_p$ . In this case, conditions (12) and (13) yield

$$A = B + 1, \quad (17)$$

$$F = E \exp(vL/D). \quad (18)$$

Employing these expression, conditions (8) and (10) can be rewritten as

$$1 + B[1 - \exp(vx_p/D)] = E[\exp(vL/D) - \exp(vx_p/D)], \quad \text{or} \\ B = \frac{E[\exp(vL/D) - \exp(vx_p/D)] - 1}{1 - \exp(vx_p/D)}, \quad (19)$$

and

$$vc_0(B - E) \exp(vx_p/D) = w_p(E[\exp(vL/D) - \exp(vx_p/D)]c_0). \quad (20)$$

Substituting (19) into (20) yields

$$\frac{vc_0[E \exp(vL/D) - E - 1]}{\exp(-vx_p/D) - 1} = w_p(E[\exp(vL/D) - \exp(vx_p/D)]c_0). \tag{21}$$

This equation can be used in order to calculate  $E$  provided the dependence of  $w_p(c)$  on  $c$  is known. Then,  $B$  and  $F$  can be expressed via  $E$  by employing (19) and (18), respectively, while  $A$  is given by (17). The reaction rate is expressed via  $E$  as

$$W = w_p(E[\exp(vL/D) - \exp(vx_p/D)]c_0). \tag{22}$$

For the first-order reaction (11), Eq. (21) and expression (22) can be rewritten as

$$\frac{E \exp(vL/D) - E - 1}{\exp(-vx_p/D) - 1} = (w_0/v)E[\exp(vL/D) - \exp(vx_p/D)], \text{ or} \tag{23}$$

$$E = \frac{1}{\exp\left(\frac{vL}{D}\right) - 1 + \frac{w_0}{v} \left[ \exp\left(\frac{vL}{D}\right) - \exp\left(\frac{vx_p}{D}\right) \right] \left[ 1 - \exp\left(-\frac{vx_p}{D}\right) \right]}, \tag{24}$$

and

$$W = w_0c_0E[\exp(vL/D) - \exp(vx_p/D)]. \tag{25}$$

Substituting (24) into (25) results in

$$W = \frac{w_0c_0[\exp(vL/D) - \exp(vx_p/D)]}{\exp\left(\frac{vL}{D}\right) - 1 + \frac{w_0}{v} \left[ \exp\left(\frac{vL}{D}\right) - \exp\left(\frac{vx_p}{D}\right) \right] \left[ 1 - \exp\left(-\frac{vx_p}{D}\right) \right]}. \tag{26}$$

Expression (26) allows one to identify analytically a few reaction regimes. If the reaction is slow, one can neglect the term proportional to  $w_0/v$  in the denominator, i.e.,

$$W \simeq w_0c_0 \frac{\exp(vL/D) - \exp(vx_p/D)}{\exp(vL/D) - 1}. \tag{27}$$

For slow and rapid diffusion with  $D \ll vL$  and  $D \gg vL$ , this expression is reduced, respectively, to

$$W \simeq w_0 \text{ and } W \simeq (x - x_p/L)w_0. \tag{28}$$

If the reaction is rapid, one can neglect the first term,  $\exp(vL/D) - 1$ , in the denominator of (26), i.e.,

$$W \simeq vc_0/[1 - \exp(-vx_p/D)]. \tag{29}$$

For slow and rapid diffusion with  $D \ll vL$  and  $D \gg vL$ , the latter expression is reduced, respectively, to

$$W \simeq vc_0 \text{ and } W \simeq Dc_0/x_p. \tag{30}$$

It is of interest to notice that according to (29) the reaction rate is larger than  $vc_0$ . Mathematically, this is directly related to condition (12) which fixes the reactant concentration but does not impose restriction on the total reactant flux at  $x = 0$ . Physically, the total flux is in this case larger than  $vc_0$  due to the reactant gradients near the channel inlet at  $x < 0^-$ .

Typical profiles of the reactant concentration and the reaction rate calculated as a function of  $w_0/v$  for the first-order reaction are shown in Figs. 2 and 3. For comparison, the concentration profile,

$$c(x) = c_0 \frac{\exp(vL/D) - \exp(vx/D)}{\exp(vL/D) - 1}, \tag{31}$$

predicted in the absence of reaction is shown as well.

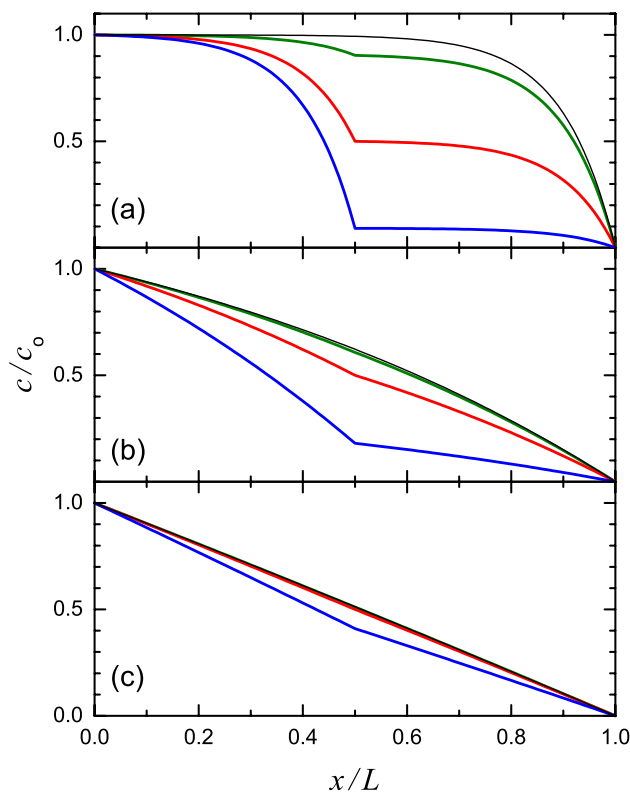
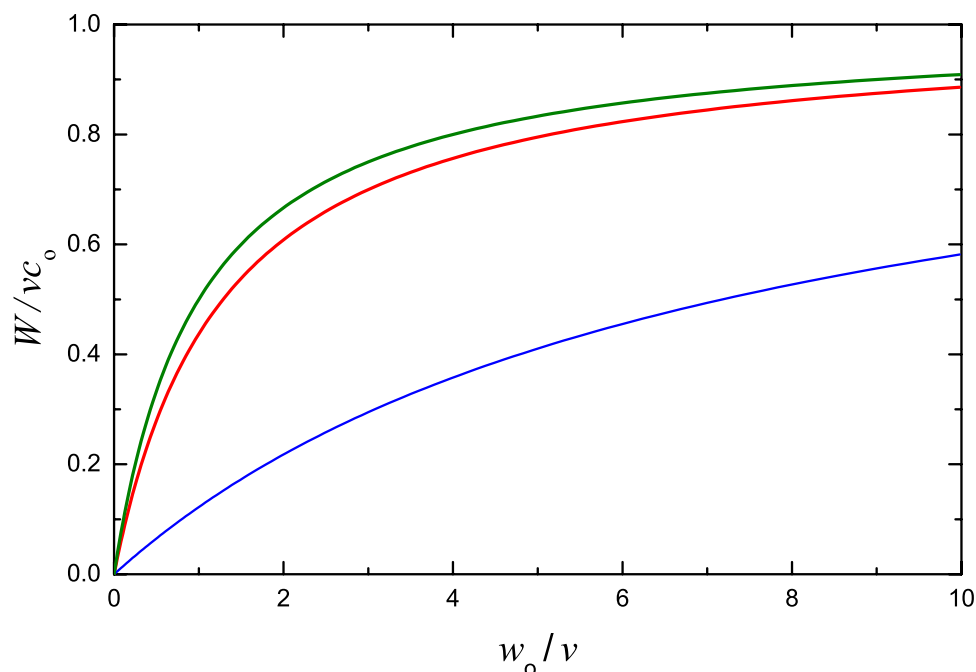


**Fig. 2** Normalized reactant concentration along the nanochannel according to the model with the Dirichlet boundary conditions: **a** slow diffusion with  $D/vL = 0.1$ , **b** moderate diffusion with  $D/vL = 1$ , and **c** rapid diffusion with  $D/vL = 10$ . In each cases, the results of calculations are shown for slow reaction with  $w_0/v = 0.1$  (upper thick line), reaction with  $w_0/v = 1$  (medium thick line), and rapid reaction with  $w_0/v = 10$  (lower thick line). A catalytic nanoparticle is located in the center of the channel ( $x_p = L/2$ ). For comparison, the upper thin line shows the concentration profile calculated in the no-reaction case (31)

**Fig. 3** Normalized reaction rate,  $W/vc_0$ , as a function of  $w_0/v$  for  $D/vL = 0.1$  (upper line), 1 (mediul line), and 10 (lower line) according to the model with the Dirichlet boundary conditions. A catalytic nanoparticle is located in the center of the channel ( $x_p = L/2$ )



## 2.5 With the Danckwerts Boundary Conditions

In this case, conditions (14) and (15) yield

$$A = 1, \quad (32)$$

$$E = 0, \quad (33)$$

and accordingly conditions (8) and (10) can be rewritten as

$$B = (1 - F) \exp(-vx_p/D), \quad (34)$$

$$vc_0 B \exp(vx_p/D) = w_p(Fc_0). \quad (35)$$

Substituting (34) into (35) results in

$$vc_0(1 - F) = w_p(Fc_0). \quad (36)$$

For the first-order reaction, this equation is reduced to

$$v(1 - F) = w_0 F, \quad \text{or} \quad F = v/(v + w_0). \quad (37)$$

With this expression for  $F$ , the reaction rate is given by

$$W = vw_0 c_0 / (v + w_0). \quad (38)$$

The related concentration profiles are shown in Fig. 4.

## 3 Conclusion

The analysis presented shows how the kinetics of reaction occurring on a single catalytic nanoparticle in a fluidic nanochannel can be described by the equation similar to that used

for PFR with dispersion. In the practically interesting case when the channel length is appreciably larger than the channel radius, the Dirichlet boundary conditions are found to be suitable. In general, the Danckwerts boundary condition(s) can, however, be suitable as well especially near the outlet. The analytical and numerical results obtained with these conditions have clarified the likely types of the profiles of the reactant concentration along the channel and the dependence of the reaction rate on the parameters.

It is of interest that despite the gradients in the reactant concentration the structure of expression (26) for the reaction rate calculated with the Dirichlet boundary conditions is similar to that for CSTR. For the Danckwerts boundary conditions, the structure of expression (38) for the reaction rate is identical to that for CSTR. To illustrate this explicitly, I recall that in the CSTR case the rate of the first-order reaction is given by

$$W = kc_0 / (1 + k\tau), \quad (39)$$

where  $k$  is the reaction rate constant, and  $\tau$  is the residence time. This analogy results from the fact that the observed reaction rate is just a balance between the local reaction rate and the reactant supply and removal to the region where a reaction takes place. For TAPR, for example, the situation is similar [2, 14]. The formal analogy between the reaction kinetics in the conventional CSTR and in the fluid channel under consideration facilitates the understanding of the reaction kinetics in the latter case.

Although the model employed is focused on the simplest 1D case with the first-order reaction, various aspects

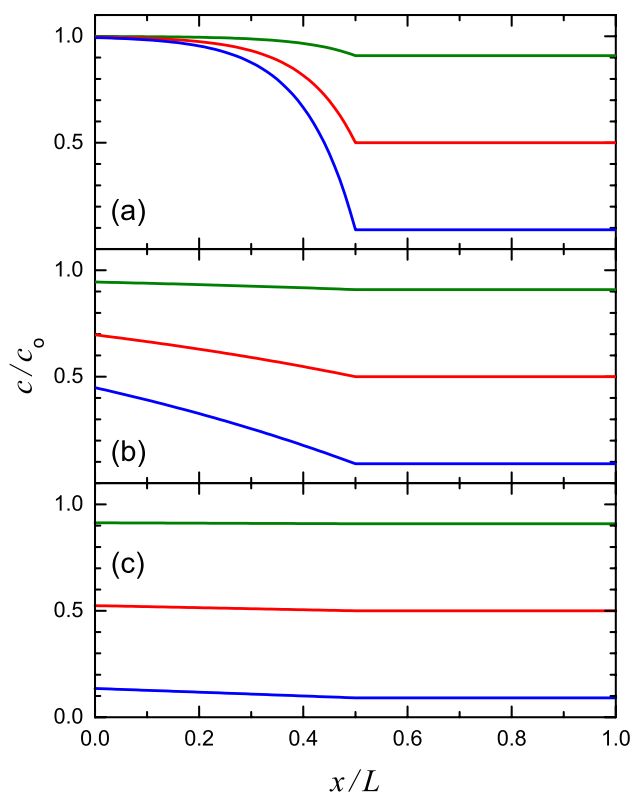


**Fig. 4** Normalized reactant concentration along the nanochannel according to the model with the Danckwerts boundary conditions: **a** slow diffusion with  $D/vL = 0.1$ , **b** moderate diffusion with  $D/vL = 1$ , and **c** rapid diffusion with  $D/vL = 10$ . In each cases, the results of calculations are shown for slow reaction with  $w_0/v = 0.1$  (upper thick line), reaction with  $w_0/v = 1$  (medium thick line), and rapid reaction with  $w_0/v = 10$  (lower thick line). A catalytic nanoparticle is located in the center of the channel ( $x_p = L/2$ ). Note that with increasing diffusion coefficient or reaction rate constant the concentration becomes appreciably smaller than  $c_0$  even near the channel inlet (at  $x = 0$ )

of the corresponding analysis (e.g., the discussion of various boundary conditions) are expected to be applicable in more complex cases. The model can easily be extended to scrutinize such cases. As a rule, it will, however, be related with numerical calculations, i.e., the results will not be generic.

Finally, I may repeat (cf. the Introduction) that the experimental studies of reactions occurring in a nanofluidic channel on a single catalytic NP are just beginning [12, 22], and I do not discuss specific experiments. The interplay between the experiment and theory is here expected to be similar, for example, to that with the studies of catalytic reactions occurring in TAPR where the first purely theoretical works focused on the corresponding 1D model (e.g., [14]) were followed by the experiments (e.g., [2]) with the interpretation based on the early developed theory.

**Acknowledgements** Open access funding provided by Chalmers University of Technology. This work was supported by Russian Academy of Sciences and Federal Agency for Scientific Organizations (Project 0303-2016-0001). The author thanks C. Langhammer for useful discussions which were behind this project.

## Compliance with Ethical Standards

**Conflict of interest** The author declares that he has no conflict of interest.

**Open Access** This article is licensed under a Creative Commons Attribution 4.0 International License, which permits use, sharing, adaptation, distribution and reproduction in any medium or format, as long as you give appropriate credit to the original author(s) and the source, provide a link to the Creative Commons licence, and indicate if changes were made. The images or other third party material in this article are included in the article's Creative Commons licence, unless indicated otherwise in a credit line to the material. If material is not included in the article's Creative Commons licence and your intended use is not permitted by statutory regulation or exceeds the permitted use, you will need to obtain permission directly from the copyright holder. To view a copy of this licence, visit <http://creativecommons.org/licenses/by/4.0/>.

## References

- Mann U (2009) Principles of chemical reactor analysis and design: new tools for industrial chemical reactor operations. Wiley, Hoboken
- Wang Y, Ross Kunz M, Siebers S, Rollins H, Gleaves J, Yablonsky G, Fushimi R (2019) Transient kinetic experiments within the high conversion domain: the case of ammonia decomposition. *Catalysts* 9:104
- Van Santen R (2017) Modern heterogeneous catalysis: an introduction. Wiley, Weinheim
- Keil FJ (2018) Molecular modelling for reactor design. *Ann Rev Chem Biomol Eng* 9:201–227
- Somorjai GA, Li Y (2010) Introduction to surface chemistry and catalysis. Wiley, Hoboken
- Ertl G (2017) Molecules at solid surfaces: a personal reminiscence. *Ann Rev Phys Chem* 68:1–17
- Freund H-J (2010) Model studies in heterogeneous catalysis. *Chem Eur J* 16:9384–9397
- Tachikawa T, Majima T (2012) Single-molecule, single-particle approaches for exploring the structure and kinetics of nanocatalysts. *Langmuir* 28:8933–8943
- Mayer KM, Shnipes J, Davis D, Walt DR (2015) Catalytic kinetics of single gold nanoparticles observed via optical microwell arrays. *Nanotechnology* 26:055704
- Alekseeva S, Nedrygailov II, Langhammer C (2019) Single particle plasmonics for materials science and single particle catalysis. *ACS Photonics* 6:1319–1330
- Ye R, Mao X, Sun X, Chen P (2019) Analogy between enzyme and nanoparticle catalysis: a single-molecule perspective. *ACS Catal* 9:1985–1992
- Fritzsche J, Albinsson D, Fritzsche M, Antosiewicz TJ, Westerglund F, Langhammer C (2016) Single particle nanoplasmonic sensing in individual nanofluidic channels. *Nano Lett* 16:7857–7864
- Nekhamkina O, Rubinstein BY, Sheintuch M (2000) Spatiotemporal patterns in thermokinetic models of cross-flow reactors. *AIChE J* 46:1632–1640

14. Phanawadeea P, Shekhtman SO, Jarungmanorama C, Yablonsky GS, Gleaves JT (2003) Uniformity in a thin-zone multi-pulse TAP experiment: numerical analysis. *Chem Eng Sci* 58:2215–2227
15. Matera P, Karsten R (2012) When atomic-scale resolution is not enough: spatial effects on in situ model catalyst studies. *J Catal* 295:261–268
16. Selmi S, Mitchell DJ, Manoranjan VS, Voulgarakis NK (2017) A hybrid fluctuating hydrodynamics and kinetic Monte Carlo method for modeling chemically-powered nanoscale motion. *J Math Chem* 55:1833–1848
17. Zhang Y (2019) Density and viscosity profiles governing nano-channel flow. *Physica A* 521:1–8
18. Danckwerts PV (1953) Continuous flow systems: distribution of residence times. *Chem Eng Sci* 2:1–18
19. Guettel R, Turek T (2009) Comparison of different reactor types for low temperature Fischer–Tropsch synthesis: a simulation study. *Chem Eng Sci* 64:955–964
20. Russo V, Salmi T, Mammitzsch F, Jogunola O, Lange R, Wærnøa J, Mikkola J-P (2017) First, second and n-th order autocatalytic kinetics in continuous and discontinuous reactors. *Chem Eng Sci* 172:453–462
21. Mott HV, Green ZA (2015) On Danckwerts' boundary conditions for the plug-flow with dispersion/reaction model. *Chem Eng Commun* 202:739–745
22. Levin S, Fritzsche J, Nilsson S, Runemark A, Dhokale B, Ström H, Sunden H, Langhammer C, Westerlund F (2019) A nanofluidic device for parallel single nanoparticle catalysis in solution. *Nature Commun* 10:4426